REVISTA MATÉRIA V.28 N.1
ISSN 1517-7076 articles e20220300, 2023

Experimental study of reinforced concrete piles wrapped with fibre reinforced polymer under vertical load

Jesudhas Prakash Arul Jose[1], Mahmoud Al Khazaleh[2], Fleming Prakash[3], Francis Michael Raj[4]

[1]Paavai Engineering College, Department of Civil Engineering. Paavai Nagar, NH-44, Pachal, 637018, Tamil Nadu, Namakkal, India.

[2]Aqaba University of Technology, Munib & Angela Masri Faculty of Engineering, Department of Civil Engineering. Ports Highway, 77110, Aqaba, Jordan.

[3]Tamil Nadu Urban Habitat Development Board. No.5, Kamarajar Salai, near Vivekananda House, Ayothiya Nagar, Triplicane, 600005, Chennai, India.

[4]Stella Mary's College of Engineering, Department of Mechanical Engineering. Aruthenganvilai, Kalluketti Junction, Azhikkal Rd, Tamil Nadu, 629202, India.

e-mail: prakasharuljose11@gmail.com, mkhazaleh@aut.edu.jo, erflemingprakash@gmail.com, michaelrajf@yahoo.com

ABSTRACT

This research mainly focuses on the nature of Fiber-Reinforced Polymers (FRP) wrapped piles for the axial compression load. Normally, the degradation of Reinforced Cement Concrete (RCC) structures occurred due to corrosion, inadequate quality materials, aging, live load increments, fatigue, damages and deterioration, and so forth. RCC pile foundations are commonly affected by the above reasons. So, these structures can be strengthened with suitable methods such as jacketing, stitching, overlaying, sealing, grouting, coating, Near Surface Mounted (NSM) systems, FRP wrapping, repairing, and blanketing. FRP wrapping is well suited for strengthening pile structures because of its easy application, and this method is done without using heavy tools and skilled labor. Due to its being non-metallic, FRP reinforcing has desirable properties such as high resistance to chemicals as well as heat, flexibility, large tensile strength, permeability, and also no oxidation. Thus, FRP wrapping was selected as the chosen approach for this ongoing research. In this study, we apply an axial compression load as well as a skin friction condition to a pile member that has been modified to assess its performance and behavior.

Keywords: Retrofit; FRP; Pile strengthening; Static vertical loads; Pile stiffness.

1. INTRODUCTION

Matrix and reinforcing fibers make up the FRP composite material. Fiber is frequently used as the reinforcing component, which modifies the FRP's stiffness and strength. Matrix resources like vinyl ester, polyester, phenolic, thermoplastic, epoxy, and so on are used to prevent fiber damage. Common names for these materials include glass fiber-reinforced plastic, carbon fiber-reinforced plastic, and aramid fiber-reinforced plastic. Fibers can also be strengthened by using other materials such as carbon, glass, Polypropylene or aramid. The strength of FRP depends on a variety of elements [1–3], including fiber composition, orientation, and matrix.

FRP has lately acquired favor around the world in civil engineering [4, 5], and engineers are confident in its application [2, 6–11] due to its many advantages. FRP is commonly utilised to reinforce internal structural parts like beams and slabs. They are also used in the construction of outside buildings like bridges, columns, foundation piles, and paved roads. Concrete-filled FRP tubes serve as the basis for FRP piles are a cutting-edge product in civil engineering [2]. The concrete center of a FRP pile is encased in a stronger FRP shell. The FRP pile's outside FRP shell offers tensile strength and corrosion protection, while the interior concrete core offers compressive strength.

Traditionally, steel, concrete, and wood piles have been used to support massive projects on land and sea. However, corrosion in hostile environments can be a problem for these materials, which is why FRP piles have become increasingly popular in geotechnical engineering in recent years [12–14]. Studies on FRP piles have been conducted, with topics including the piles' structural behavior, the features of different FRP kinds, and the piles' corrosion resistance [15–29]. The soil condition is an essential component that must be addressed for FRP piles because piles are used to support massive constructions, yet most of the works discussed over FRP piles and do not include soil effects. In reality, there are fewer studies on FRP heaps than

Corresponding Author: Francis Michael Raj Received on 15/11/2022 Accepted on 28/12/2022

DOI: https://doi.org/10.1590/1517-7076-RMAT-2022-0300

on traditional piles [30–36], and even fewer studies evaluate the influence of soil when examining FRP piles. The research among FRP piles with varying load regimes is not necessary, leaving a gap [35]. Furthermore, due to their relative lack of rigidity, FRP piles necessitate greater care during construction than traditional piles. FRP pilings are limited in their use because there are no established regulations for their installation [2]. However, there is a growing need for FRP pile construction that prioritizes both safety and efficiency. The goal of this experimental investigation is to help engineers make better judgments that lead to more efficient building instructions by determining what influences the performance of FRP piles in sandy soil under the axial and lateral stresses.

In the current investigation, static analysis on RC piles strengthened using FRP wrapping and various confinements are conducted to research the behavior of piles as well as their contact with soil mass. This analysis relies on the estimated strength parameters of soils. Though quite a several researchers have been done related to the performance analysis of axially loaded piles, no work has reported the behavior of FRP-wrapped RC piles. Hence it was decided to carry out extensive experimental work to explore the behavior of axially loaded piles with FRP wrapping and its interaction with the soil.

2. MATERIALS AND METHODS

The substances that are used for making concrete were investigated before casting the samples according to the provisions of relevant Indian Standard codes. Sankar 43 grade OPC manufactured by the India Cements industry at Sankar Nagar (TamilNadu) has been used throughout the analysis and was utilized for making the samples. The fine aggregate used is mostly fresh as well as natural river sand complying to would be: 383 – 1970. Hard Blue Granite angular coarse aggregate of 10 mm size has been conforming to IS383-1970. The diameter and dimension of reinforcement were chosen based on IS: 1786–1985. A Universal Testing Machine was employed to test the tensile stress of the rebar of 6 mm diameter. The reinforcement region is less for high-strength concrete steel piles. In this investigation, Fe 415 steel from Trichy Steel Rolling Mills has been used. The residual water acts as a lubricant within the coarse and fine aggregates there by making the concrete feasible. For hydration, cement needs almost three by tens of its mass of water. Therefore, the least water content proportion needed is 0.38. In this analysis, IS process was applied for the design of mixes of grade M30. All the mixes were designed based on the grade of control mentioned as “good” in the IS code.

2.1. The casting of specimens

The samples are obtained as a result of casting for one day in molds made of steel. After casting, the demoulded specimens are treated in water curing. After adequate curing, prepared concrete samples are wrapped with fiber-reinforced polymers by following the steps given below. Table 1 presents the mix proportions from the mix design.

The prepared concrete base specimens are rubbed using silicon carbide sheets of water-proof paper to remove the presence of any deleterious and loose materials found in the base. The component such as resin and hardener are used to make the saturant system was high melting point and so thermally strong that was used in this research. These components are prepared manually by mixing them with hands for 3 minutes of the application. The priming surface was coated with an initial saturant coating, and the FRP layer was contained on the surface. Surrounding the concrete specimens were FRP layers. This wrapping over laps (¼)th of the concrete specimen perimeter to avoid fiber deboning or sliding during testing. Further, this will ensure the improvement of full strength. The flexure and compression strength of concrete was estimated by casting beam prisms (10 cm × 10 cm × 50 cm), and standard cubes (15 cm × 15 cm × 15 cm) respectively. This casting is done by using iron molds. Further, cylindrical samples of 150 mm diameter and 300 mm height were also cast for calculating the compressive and tensile strength, splitting, etc. Proper measures were made to ensure that no bulging or distortion of mold occurred during the compaction with the vibrator. Thirteen pile samples of 50 mm diameter and 750 mm height, four long cylinders of 30 cm length and 15 cm diameter, six standard cubes of 150 mm size, and three beam prisms of 100 mm × 100 mm × 500 mm were also cast by using the M30 mix. Upon completion of the initial curing period of 24 ± ½ hours, these materials are demoulded and given a further 28 days to fully cure. The cured specimen was removed from the incubator and stored to wait further testing.

Table 1: Mix proportions from mix design.

GRADE	TARGET MEAN STRENGTH (N/mm^2)	W/C RATIO	MIX PROPORTION (C:FA:CA:W)	REMARKS
M30	38.25	0.385	1:1.05:2.56:0.39	IS method

3. RESULTS AND DISCUSSION

3.1. Loading of piles

In general, piles are necessary to handover the vertical loads to the surrounding soil media. The same trend that was presented as a substitute for the piles in the deep foundation field is FRP composite materials. The different FRP composite materials are given as:

- Bidirectional pile confined with AFRP sheets (Bi-AFRP)
- Bidirectional pile confined with PFRP sheets (Bi-PFRP)
- Unidirectional pile confined with CFRP along the circumference (Uni-CFRP-C)
- Unidirectional pile confined with CFRP along the length (Uni-CFRP-L)
- Unidirectional pile confined with GFRP along the circumference (Uni-GFRP-C)
- Unidirectional pile confined with GFRP along the length (Uni-GFRP-L)
- Unidirectional pile confined with BFRP along the circumference (Uni-BFRP-C)
- Unidirectional pile confined with BFRP along the length (Uni-BFRP-L)

The experimental analysis provides the characteristics of unconfined piles and FRP wrapping allowed for vertical loading. Three different surface RC piles remained covered using similar strengthening materials to examine the performance of RC piles having FRPs allowed to carry vertical loads. Factors that differ in the analysis include wrapping ingredients such as aramid, basalt, and carbon as well as glass and fiber orientations towards the circumference and length.

3.2. Piles unconfined and confined with different FRPs

Experimental analysis was performed with eleven piles. Of these, only three piles are investigated without wrapping and the remaining eight piles are investigated after wrapping with different configuration FRP composites. Concrete piles with different surface roughness and wrapped with various FRP composites are given in Figures 1 and 2.

3.3. Load carrying capability in piles

The capacity of a pile, or its Cup, is defined as how much weight it can support before sinking. The safe load is the maximum load Qa that can be properly supported by such a pile, which is determined by the following criteria: (a) the ratio of the ultimate bearing resistance towards the appropriate safety factor, (b) the acceptable settlement, and (c) the overall reliability of the pile foundation.

3.3.1. Dynamic formulae

The total driving energy of a hammer while hitting the hammer at the surface of the pile is equivalent to the mass of the hammer times the altitude of stroke or drop. In the case of double-acting hammers, the steam pressure will impart some energy while returning the stroke. The dynamic formulae are dependent on the work done on pile penetration and several losses that consumes the total downward energy. It is also expected that soil resistance of dynamic pile penetration is similar to the pile penetration under sustained or static loading. Some of the commonly used dynamic formulae are listed below.

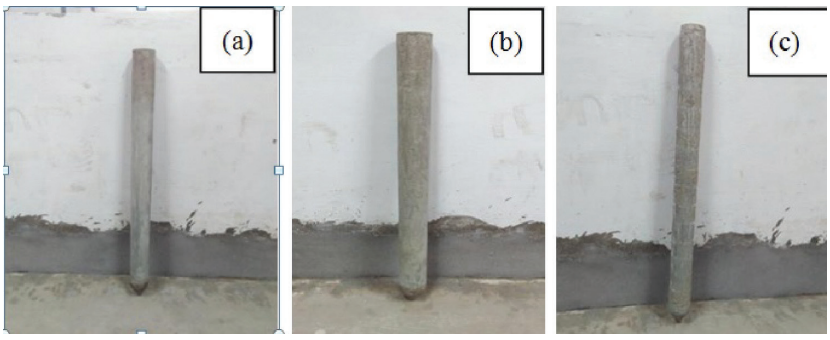

Figure 1: Concrete piles with various surfaces (a) smooth (b) medium (c) rough.

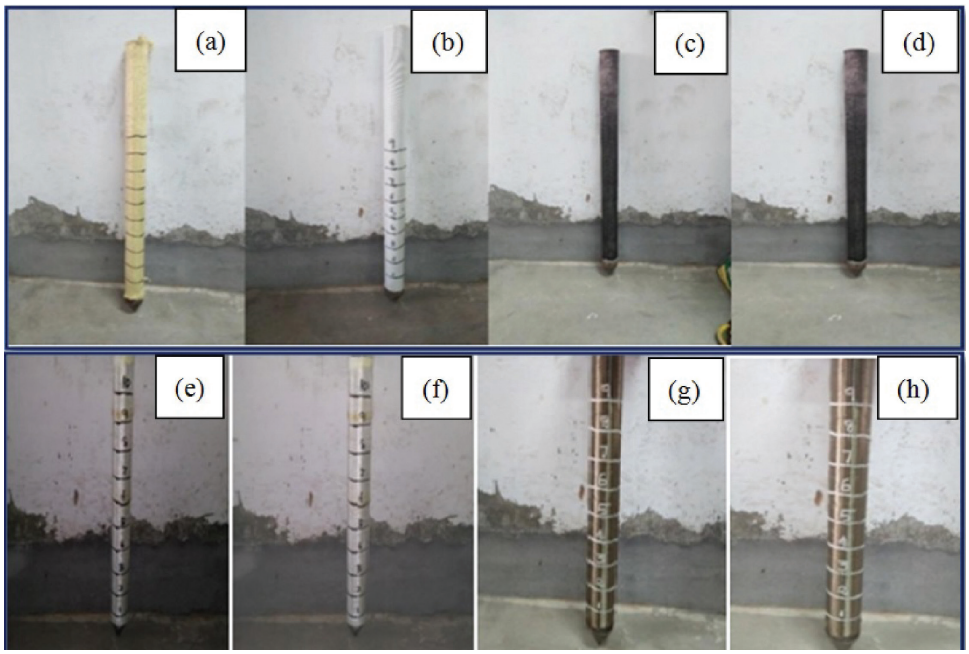

Figure 2: Concrete piles wrapped with FRP composites materials (a) Bi – AFRP (b) Bi – PFRP (c) Uni-CFRP-C (d) Uni-CFRP-L (e) Uni-GFRP-C (f) Uni-GFRP-L (g) Uni-BFRP-C (h) Uni-BFRP-L.

3.3.2. Engineering news equation

The general form of engineering news formulae was given as:

$$Qa = WH / (F(S + C)) \quad (1)$$

Where, *Qa* = Allowable load

C = Empirical constant

C = 2.5 cm for drop hammer and

C = 0.25 (single and double-acting hammer)

It is called a single-acting hammer if it is elevated by some other force (such as compressed air, internal combustion, or steam) but falls under the sole influence of gravity. Its energy is proportional to the product of the ram's mass and the height at which it falls. To lift the ram and quicken the descending stroke, it makes use of air or steam pressure. After receiving a series of quick punches, it takes off. The drop hammer refers to the hammer that is hoisted up by a winch and then permitted to fall by gravity onto pile top.

F = Safety factor = 6

S = Final set (penetration) per blow, generally taken as mean penetration cm per blow for the last 5 blows of the hammer or 20 blows of the steam hammer.

W = Hammer weight

H = Dropping height

3.4. Experimentation of RC pile

The RC pile experimental configuration is given in Figure 3.

3.4.1. Pile-driven formulae depending on safe load

Hammers which are carried by arcane or specific device called pile drivers are frequently used to operate the piles. During pile operations, items like caps, heads, or helmets were utilized to deflect hammer strikes and protect the pile head. Pile heads can be shielded from damage by inserting a padding of materials, hardwood, or rope seen between the drive cap and the pile head. For pounding large piles into hard or compacted soil, single-action hammers are the way to go. Double-acting hammers, on the other hand, are typically used to keep driving moderate or illumination piles through medium-resistance soils. The majority of piles are hammered to a resistance calculated by the quantity of blows necessary to drive them the last centimeter. The commonly specified resistances of concrete piles are 3 to 5 blows per cm. The final set penetration per blow of the drop

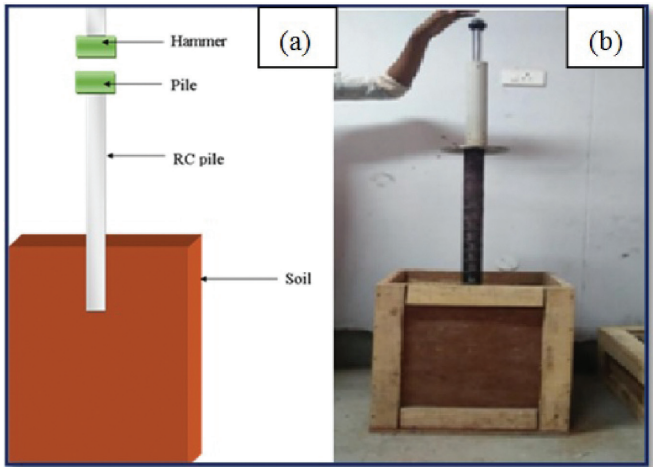

Figure 3: Experimental setup (a) schematic diagram (b) photograph.

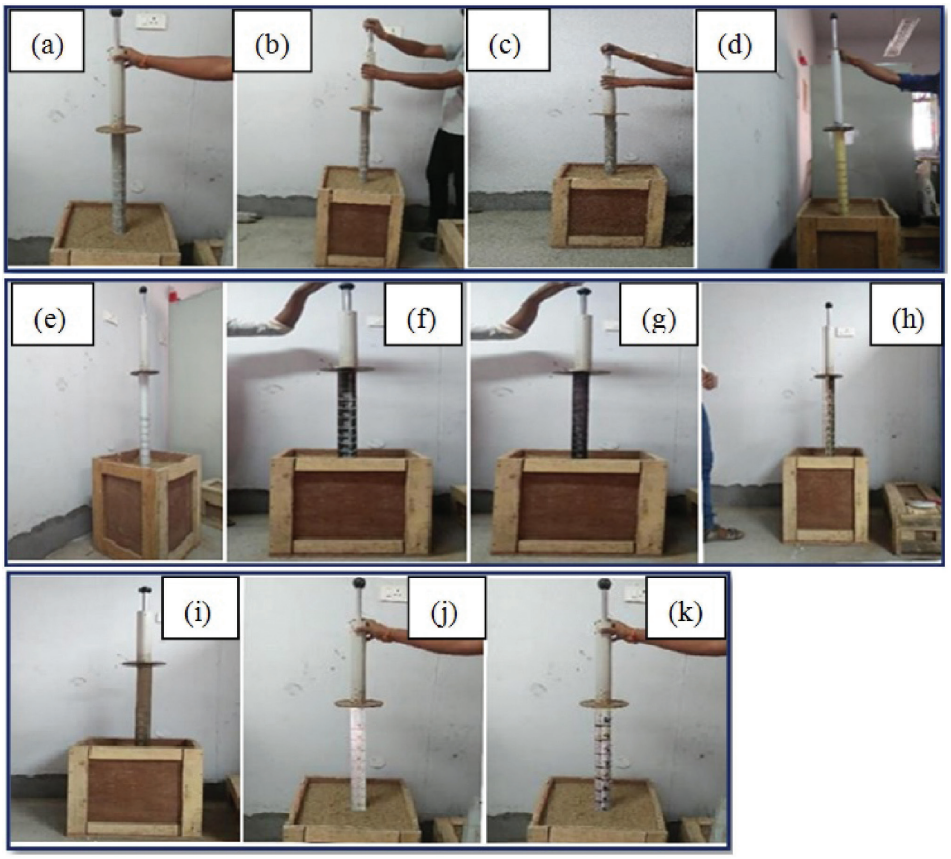

Figure 4: Types of confinement in sandy soil (based on a pile-driven formula) (a) smooth (b) medium (c) rough (d) Bi-AFRP (e) Bi-PFRP (f) Uni-CFRP-C (g) Uni-CFRP-L (h) Uni-BFRP-C (i) Uni-BFRP-L (j) Uni-GFRP-C (k) Uni-GFRP-L.

hammer or steam hammer such as the last 5 blows or 20 blows respectively is called the average penetration per blow and it is represented by S.

3.4.2. Safe load using formulas driven by pile (sandy soil)

A hammer's driving energy is proportional to its mass multiplied by the height of its stroke or drop when it strikes a pile. In the particular instance of double-acting hammers, the steam stress has also transferred some vitality even during stroke return. The soil resistances of dynamic penetration piles are expected to be equal to the piles penetrating under sustained or static loading. Various types of confinements are presented in Figure 4. The quantities of blows during the final 5 cm of penetration are shown in Table 2.

3.4.3. Safe load using formulas driven by pile (sandy clay)

The total driving energy of a hammer hitting the pile is proportional to the product of the hammer's weight and the drop or stroke length. During stroke return, an assumption is made that the steam pressure will impart some energy in the double-acting hammers. The soil resistance dynamic pile penetration is equal to the static loading pile penetration. Table 3 presents the safe load based on sandy clay pile-driven formulae. Figure 5 gives the plot of roughness versus the safe load of piles. In Figure 6 represents the types of confinements in sandy clay soil.

Table 2: Number of blows for last 5 cm penetration (sandy soil).

CONFINEMENT TYPES	NO. OF BLOWS
Uni-CFRP-L	33
Uni-CFRP-C	34
Uni-BFRP-L	37
Uni-BFRP-C	38
Uni-GFRP-L	41
Uni-GFRP-C	42
Unconfined pile-Smooth	45
Unconfined pile-Medium	47
Bi-AFRP	47
Bi-PFRP	82
Unconfined pile-Rough	280

Table 3: Pile-driven formulas for safe load (sandy soil).

TYPES OF CONFINEMENT	SAFE LOAD (N)
Uni-CFRP-L	330.79
Uni-CFRP-C	331.97
Uni-BFRP-L	343.06
Uni-BFRP-C	344.72
Uni-GFRP-L	354.53
Uni-GFRP-C	356.93
Unconfined pile-Smooth	364.44
Unconfined pile-Medium	366.11
Bi-AFRP	368.66
Bi-PFRP	423.49
Unconfined pile-Rough	492.07

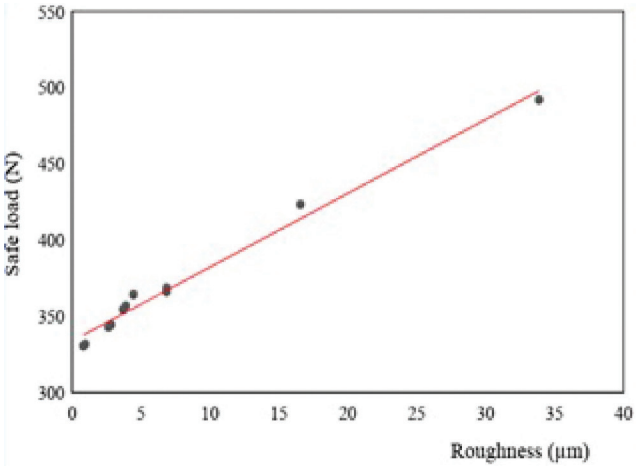

Figure 5: A pile-driven safety formula for determining safe load (sandy soil).

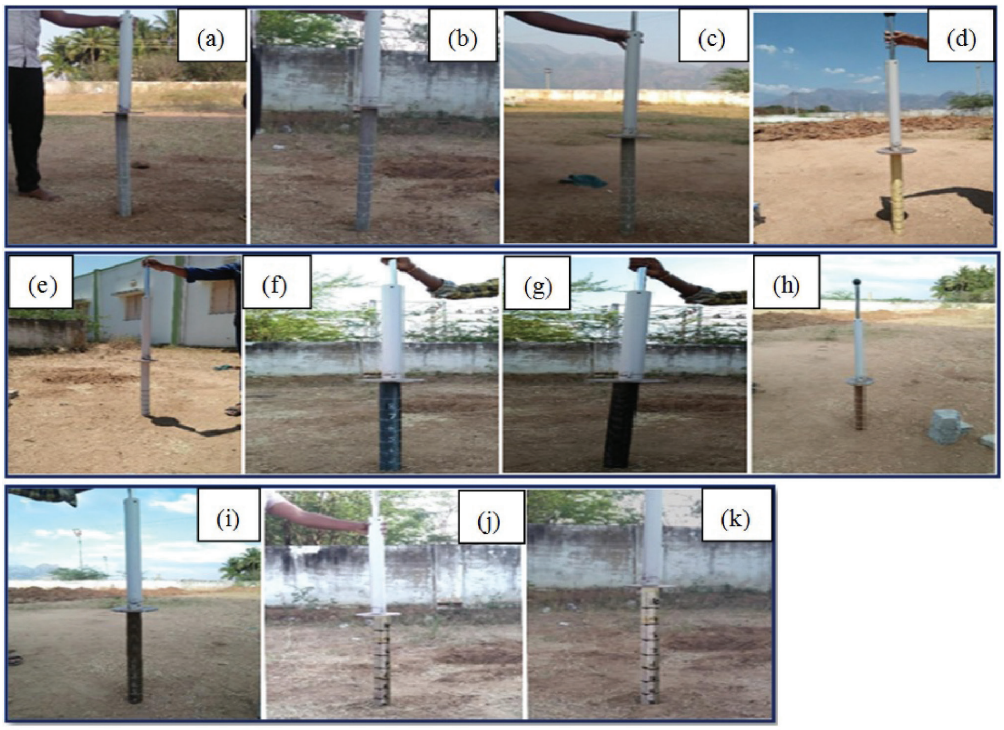

Figure 6: Types of confinement in sandy clay (based on pile-driven formulae) (a) smooth (b) medium (c) rough (d) Bi-AFRP (e) Bi-PFRP (f) Uni-CFRP-C (g) Uni-CFRP-L (h) Uni-BFRP-C (i) Uni-BFRP-L (j) Uni-GFRP-C (k) Uni-GFRP-L.

3.5. Pile load test

Sand as well as sandy clay soils of varying pile surface roughness are used in the pile load test. The surface roughness is formed by pasting the FRP wrappings as indicated in Figure 7. Sandy soil is used to maintain the uniform density of the tank with a size of 0.5 m × 0.5 m × 1 m. Further, these free-falling sand particles may vary the density of the tank. The pile testing was carried out either on the working pile which creates the structure foundation or on the test piles as shown in Tables 4 and 5. The test load is located on the head of the pile projecting above the earth level with the help of a calibrated jack attached over a rigid square or circular plate. These loads are applied repeatedly, with each application representing around a fifth of the theoretical maximum. After the maximum load is attained, the piles are no longer used in the test. The system setup of pile load testing is given in Figure 8.

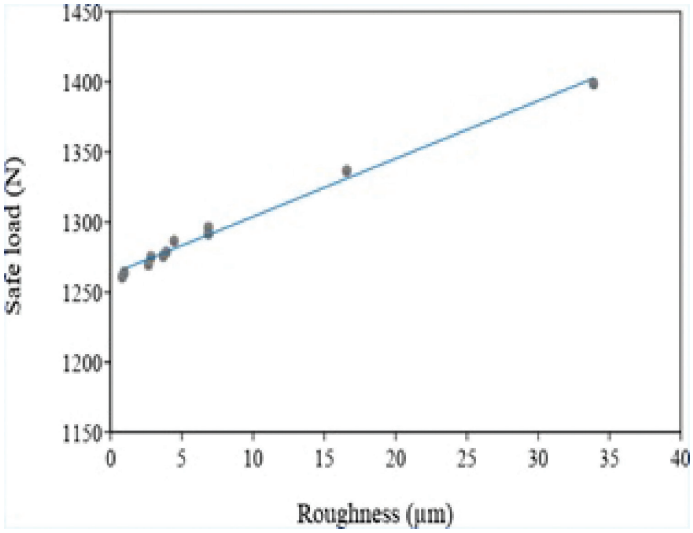

Figure 7: Safe load based on pile-driven formulae (sandy clay).

Table 4: Number of blows for last 5 cm penetration (sandy clay).

CONFINEMENT TYPES	NO. OF BLOWS
Uni-CFRP-L	139
Uni-CFRP-C	142
Uni-BFRP-L	147
Uni-BFRP-C	153
Uni-GFRP-L	153
Uni-GFRP-C	156
Unconfined pile-Smooth	165
Unconfined pile-Medium	172
Bi-AFRP	177
Bi-PFRP	253
Unconfined pile-Rough	642

Table 5: Based on pile-driven formulae, a safe load (sandy clay).

CONFINEMENT TYPE	SAFE LOAD (N)
Uni-CFRP-L	1260.88
Uni-CFRP-C	1263.92
Uni-BFRP-L	1269.61
Uni-BFRP-C	1275.01
Uni-GFRP-L	1275.69
Uni-GFRP-C	1278.44
Unconfined pile-Smooth	1286.39
Unconfined pile-Medium	1286.39
Bi-AFRP	1295.81
Bi-PFRP	1336.51
Unconfined pile-Rough	1398.51

Figure 8: Pile load test.

3.5.1. Vertical load application

In vertical load applications, the pile loads are vertically loaded above the ground surface. Through vertical loading conditions, the loads are placed between the supports of the piles. Then the behavior of the piles was observed through the head of the piles. The applied RC pile loads are measured using a dial gauge. The vertical loads of the piles are measured by mounting a 0.01 mm accuracy dial gauge. The dial gauge was mounted back to the loading point. The vertical loads are applied to the piles above the ground level through vertical loading conditions between the supporting. The pile reaction is estimated from the pile head. A dial gauge is utilized to calculate the applied RC pile loads. The test load is placed with the help of a calibrated jack mounted over a rigid square or circular plate on the tip of the pile which is projecting above the earth level. The applied load is equivalent to one-fifth of the calculated allowable load. A 0.02 sensitive dial gauge is used to record the settlements. While increasing the loads, the loads are placed for a specific amount of time until the settlement rate becomes 0.02 mm/hour. Also, these pile testing loads were loaded till reaching ultimate load condition.

3.6. The effects of vertical loads on enclosed and open RC piles (sandy soil)

Experimental analyses have been performed on 11 piles. Out of these, three piles are taken as reference piles and are tested without jacketing with FRP composites. The remaining 8 piles are tested after jacketing with FRP composites of different configurations. The different FRP types of confined and unconfined materials are shown in Figure 8. The vertical load test was accomplished concerning IS 2911 (Part 4) –1985. Vertical pile loadings were computed for each level of loading. The pile settlement versus vertical load plots is presented in Figures 9–11 and the vertical loads at settlements such as 5 mm and 12 mm that are calculated from these figures are tabulated in Table 6. Based on IS: 2911 (Part4) –1985, 50% of the final load is taken as a safe load. At this point, the overall settlement is increased to 12 mm or the final load where the load settlement reaches 5 mm at the ground surface. The minimum of one of these values is taken as the safe load of the pile.

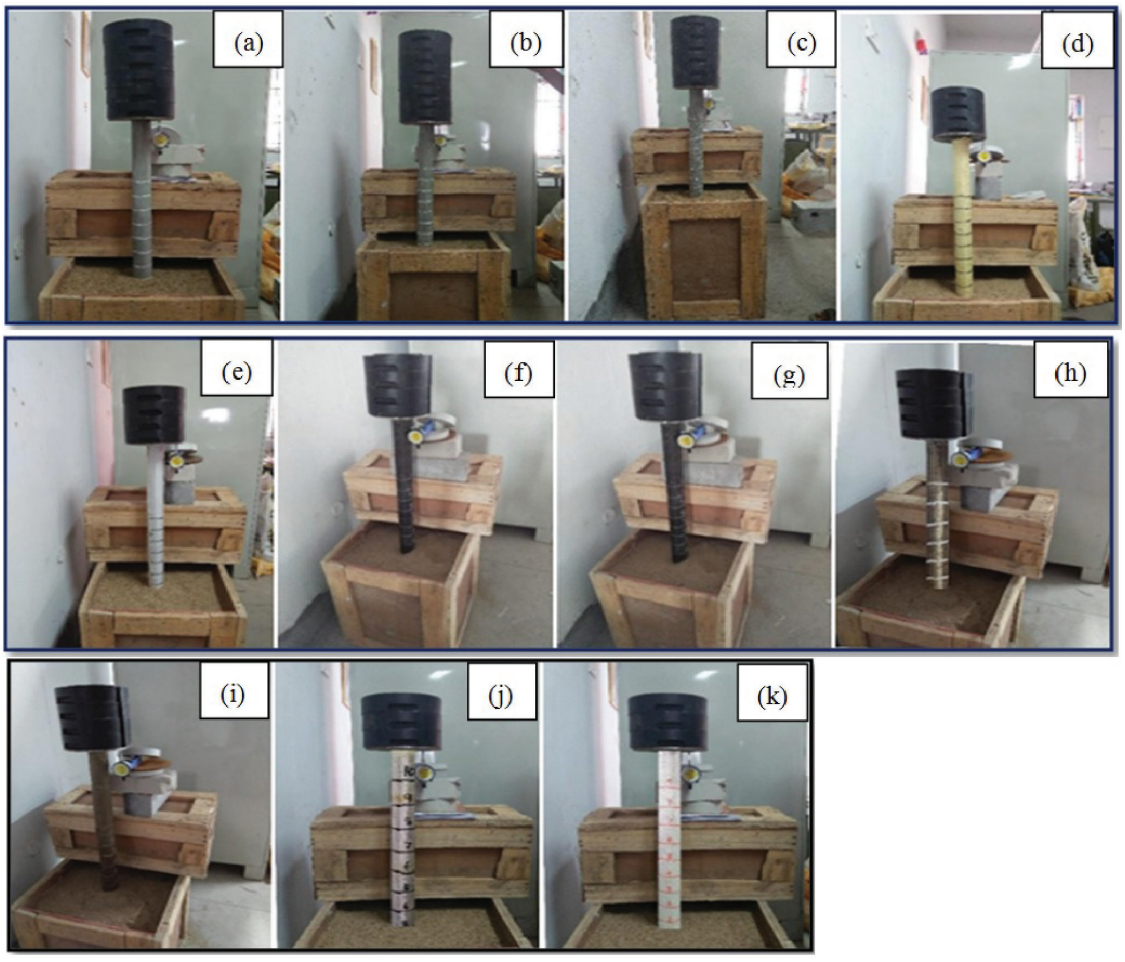

Figure 9: Types of confinement (in sandy soil) (a) smooth (b) medium (c) rough (d) Bi-AFRP (e) Bi-PFRP (f) Uni-CFRP-C (g) Uni-CFRP-L (h) Uni-BFRP-C (i) Uni-BFRP-L (j) Uni-GFRP-C (k) Uni-GFRP-L.

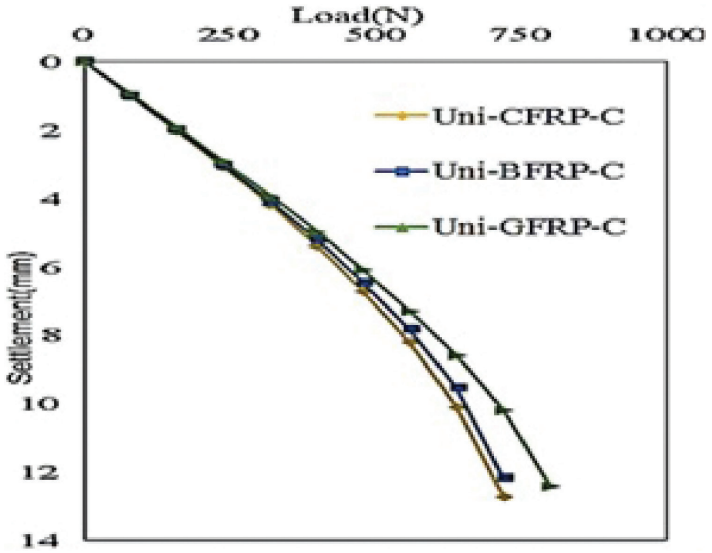

Figure 10: Load carrying capacity of FRPs orientation along the circumference (sandy soil).

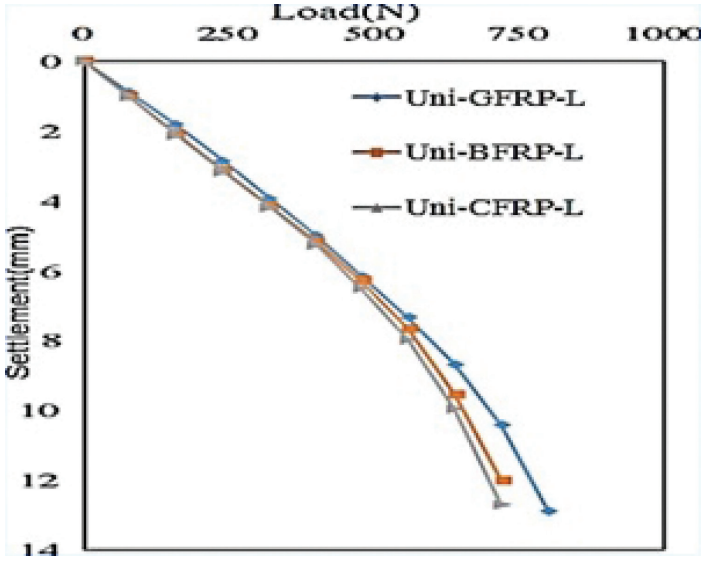

Figure 11: Vertical load carrying capacity of FRPs orientation along the length (sandy soil).

Table 6: Safe weight according to settlement standards (sandy soil).

SPECIMEN ID	LOAD EQUIVALENT TO 5 mm SETTLEMENT AT GL (N)	LOAD EQUIVALENT TO 12 mm SETTLEMENT AT GL (N)	SAFE LOAD (N)
Uni-CFRP-L	361.656	687.991	348.985
Uni-CFRP-C	363.182	689.244	349.622
Uni-BFRP-L	375.982	718.674	355.372
Uni-BFRP-C	378.488	719.856	355.980
Uni-GFRP-L	389.571	775.271	383.690
Uni-GFRP-C	392.547	745.873	385.466
Unconfined pile-Smooth	401.947	764.683	378.436
Unconfined pile-Medium	413.483	762.846	381.923
Bi-AFRP	417.493	772.656	386.873
Bi-PFRP	479.232	899.376	454.687
Unconfined pile-Rough	556.228	1063.212	537.601

3.6.1. The ability of FRP confined as well as unconfined RC piles to support structural load (sandy soil)

The changes detected in the safe vertical load capacity of various FRP-confined piles are shown in Figure 12. From experimental analysis, it is clear that the capacity of vertical loads in unconfined piles is larger than the FRP confined piles irrespective of the type of confinement used. The load transfer capacity of composites such as BFRP, CFRP, and GFRP was analyzed based on the alignment of fibers beside the dimension and perimeter of piles.

Through this analysis, it was detected that the load-carrying capacity is higher for fibers oriented along the circumference than along the length. Also, the load-bearing capacity of PFRP fibers is larger than that of AFRP fibres.

On analyzing the vertical load-carrying capacity of confined FRP piles concerning fiber orientation, there is a 1% increase in bearing capacity between circumferential and longitudinal fibres. The vertical load-bearing capacity of the FRP mat confined piles having fiber orientation having circumference and piles length has increased to 7–13%. The vertical load-bearing capacity of piles confined with PFRP composites with bi-directional piles has detected 16.73% more vertical load capacity than the piles confined with other composites.

3.7. RC piles (enclosed and unenclosed) under vertical loading (sandy clay)

Eleven piles were taken for experimental analysis of these 11piles, 3 piles are considered reference piles, and they are tested without covering with any FRP composites. The remaining 8 piles are covered with FRP composites of different configurations. The RC piles of confined and unconfined FRP composites are shown in Figure 13. For vertical loading conditions, the load test was done concerning IS 2911 (Part4) – 1985. The performance of piles is noted at each stage of loading. Figures 14–16 shows the plot of vertical loads versus pile settlement. From these plots, the vertical load settlement corresponds to 5 mm and 12 mm settlement as shown in Table 7. Based on IS: 2911(Part 4) – 1985, 50% of the final loads were considered as safe load of piles. At this point, this overall defrayal is either increased as 12 mm / the final load where these load settlement reaches 5 mm above the ground surface. However, the minimum value is considered as safe load piles which mostly occur with the first condition.

3.8. Vertical load carrying capacity of FRP confined and vertically loaded, unrestrained RC piles (sandy clay)

Figure 17 presents the changes in the vertical load-bearing capacity of piles confined with various FRP composites. Irrespective of the ways of confinement, its load-bearing capability of piles confined with FRPs was larger that of unconfined piles. For composites like BFRP, CFRP, and GFRP, the fiber orientation towards the circumference of piles has a greater load-bearing capability than the fiber orientation toward the length of piles. The load-bearing capability of PFRP fibers is larger than that of AFRP fibers. Further, fibers oriented towards the circumference of fibres in FRP confined piles can support 1% greater weight than those facing in the opposite direction. The percentage increase in the load-bearing capacity of vertically loaded piles for both

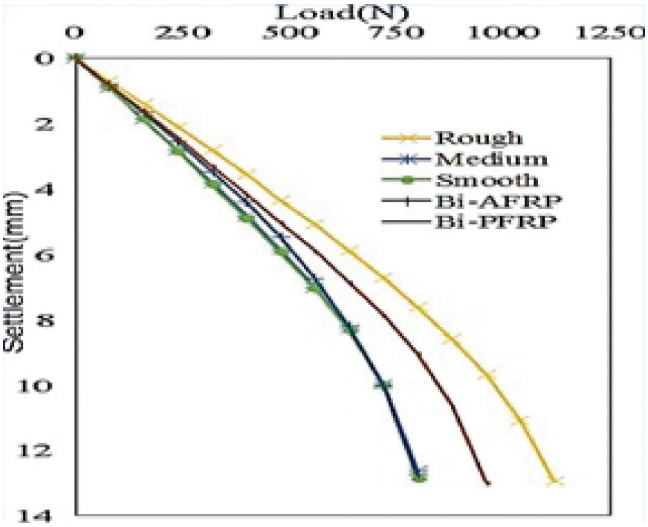

Figure 12: Vertical load carrying capacity of confined and unconfined piles (sandy soil).

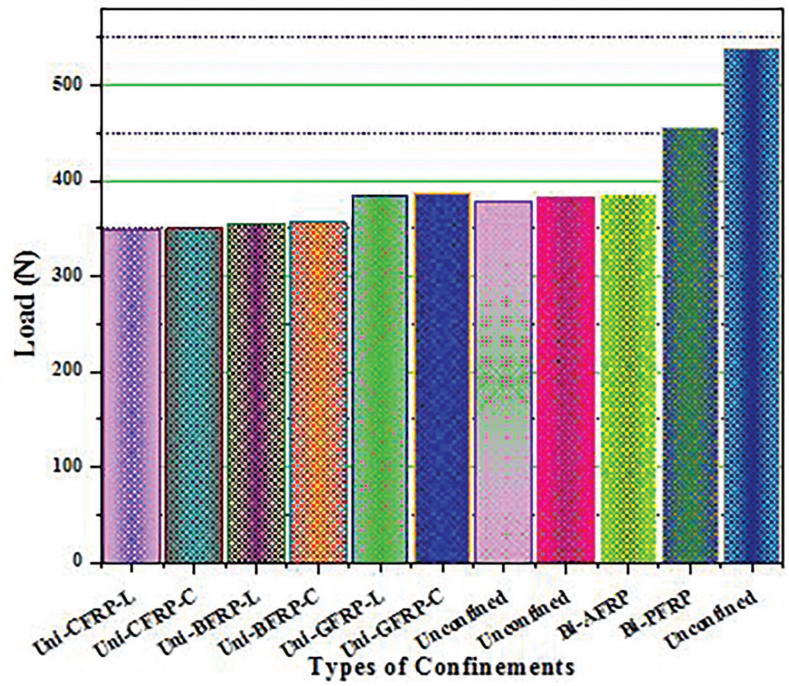

Figure 13: Safe weight according to settlement standards (sandy soil).

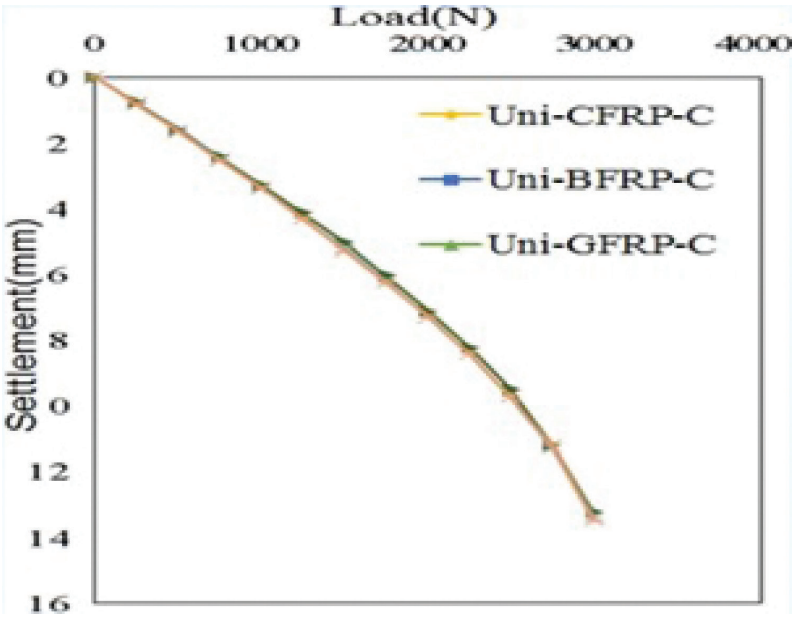

Figure 14: Load carrying capacity of FRPs orientation along the circumference (sandy clay).

the fibers oriented along the circumference and length was found to be 2–4%. The piles that are bi-directionally confined with PFRP composites revealed 4.2% more vertical load-bearing capacity compared to the piles confined with other composites.

The behavior of FRP-confined RC piles which are subjected to vertical loading conditions was observed through eleven RC piles as shown in Figure 18. The analysis concluded as unconfined piles vertical load-carrying capacity was enhanced than confined piles. Additionally, this load-bearing capacity of rough surface concrete piles is comparably higher than other RC piles. For composites such as GFRP, BFRP, and CFRP, the load-bearing capacity is higher for fibers oriented along the circumference than the fibers oriented along the length. Furthermore, the load-bearing capacity of PFRP composites is higher than that of AFRP fiber.

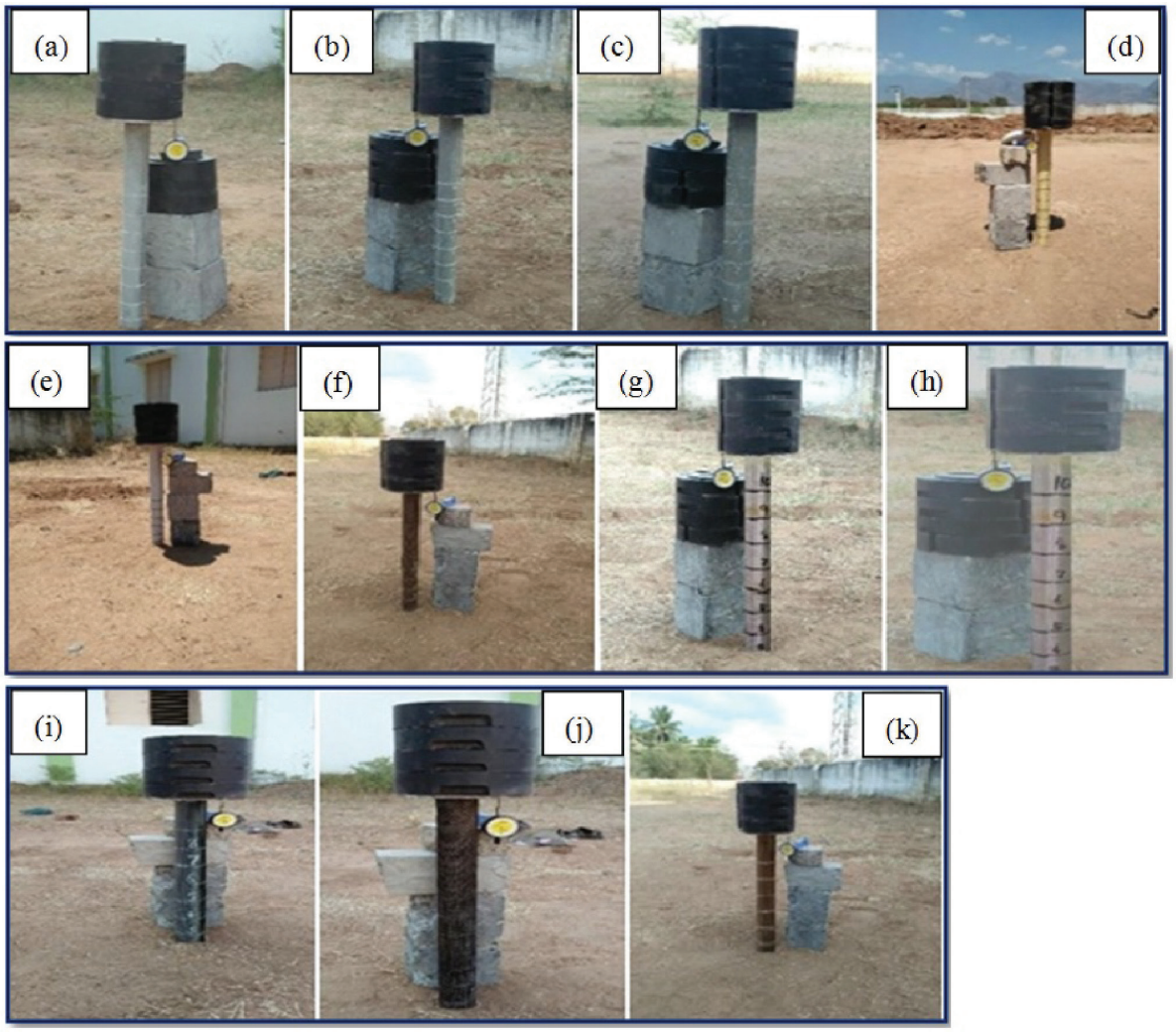

Figure 15: Types of confinement (in sandy clay) (a) smooth (b) medium (c) rough (d) Bi-AFRP (e) Bi-PFRP (f) Uni-CFRP-C (g) Uni-CFRP-L (h) Uni-BFRP-C (i) Uni-BFRP-L (j) Uni-GFRP-C (k) Uni-GFRP-L.

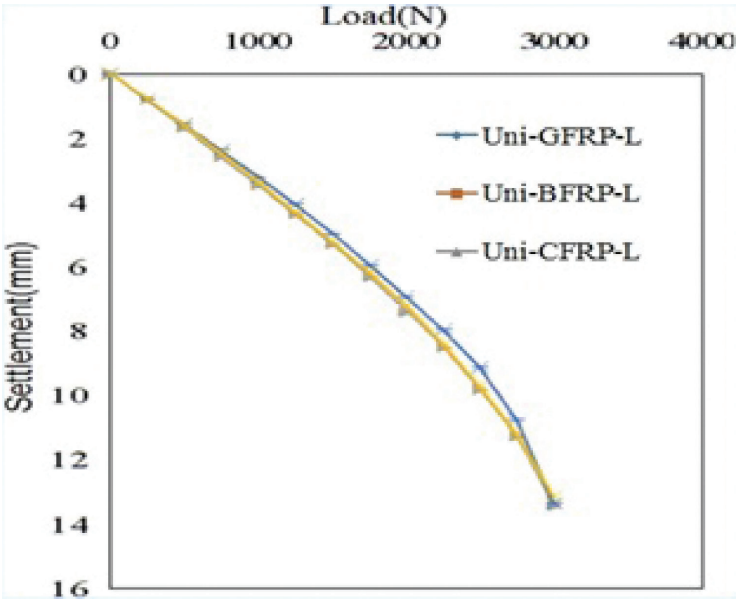

Figure 16: Load carrying capacity of FRPs orientation along the length (sandy clay).

Table 7: Settlement-based criterion for safe loading (sandy clay).

CONFINEMENT	LOAD EQUIVALENT SETTLEMENT OF 5 mm GL (N)	LOAD EQUIVALENT TO 12 mm SETTLEMENT AT GL (N)	SAFE LOAD (N)
Uni-CFRP-L	1374.381	2709.522	1364.761
Uni-CFRP-C	1378.894	2718.557	1369.274
Uni-BFRP-L	1388.7230	2746.215	1378.105
Uni-BFRP-C	1396.159	2751.018	1375.5090
Uni-GFRP-L	1398.121	2757.002	1378.5010
Uni-GFRP-C	1403.713	2764.262	1382.1310
Unconfined pile-Smooth	1414.994	2784.864	1392.432
Unconfined pile-Medium	1423.235	2794.420	1397.210
Bi-AFRP	1431.82	2816.647	1408.3235
Bi-PFRP	1480.82	2912.589	1456.2945
Unconfined pile-Rough	1552.334	3047.771	1523.8855

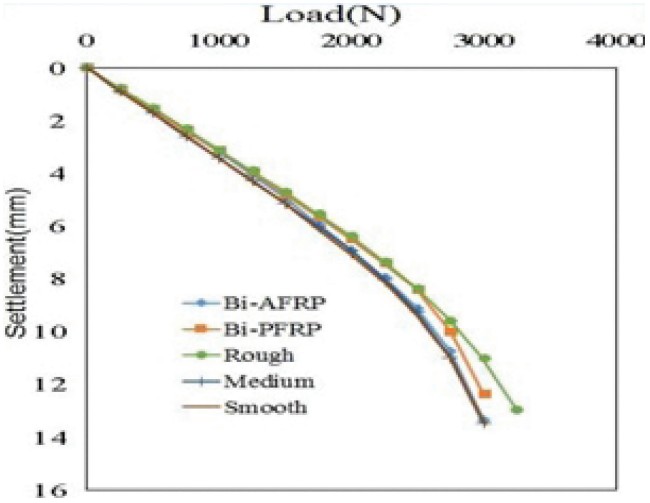

Figure 17: The capability of confined as well as unconfined piles to support loads (sandy clay).

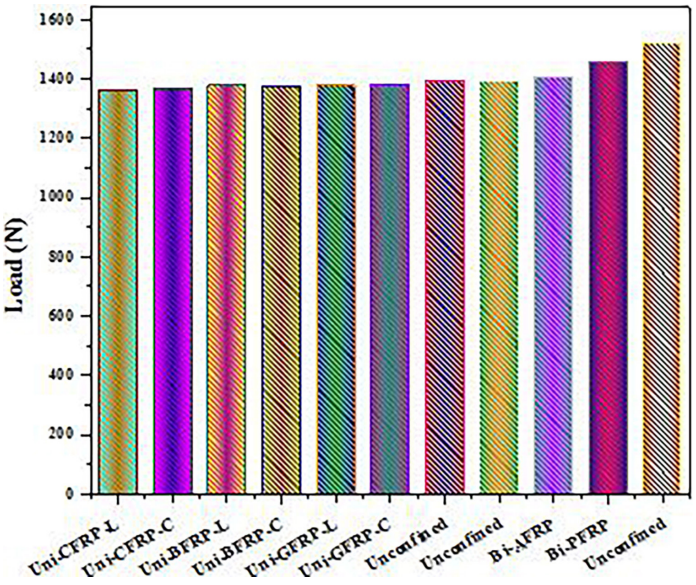

Figure 18: Settlement-based criterion for safe loading (sandy clay).

4. CONCLUSIONS

Under vertical loading conditions, the confinement effects of FRP composites while increasing the vertical resistance of pile foundations were analyzed through the existing case studies and analytical methods. The advantage of using FRPs in pile foundation retrofitting is dependent on the capability of these composites to maintain their chemical and mechanical characteristics during the application. The stability and strength of geotechnical structures depend on the response of the soil-soil interface. A direct shear test was applied to find the interface friction angle at FRP-jacketed concrete specimens and soil. Subsequently, the responses of FRP-soil were equated with the concrete-soil.

Both the durability and durability of the foundation design are affected by the soil-solid interface reaction. The friction angle seen between the soil as well as FRP concrete is measured directly by shear testing. In terms of soil type & grading, fiber species (aramid, basalt, carbon, and glass), as well as fiber orientation (with regards to shear loading), the practical study revealed that the interfacial angle varies greatly (parallel, perpendicular, both parallel and perpendicular) and surface roughness of specimens (rough, medium and smooth). The shear strength interface is improved by increasing the surface roughness of the specimen. The interface friction angle was enhanced if these shear force's direction was perpendicular to the fiber's alignment. According to the data collected in the experiments, the roughness of such piles' surfaces has a major impact on their load-bearing capacity. For example, if the pile's surface morphology is increased, its load-bearing capacity will likewise rise. Also, the load-bearing capacity improves if fiber is directed around the piles rather than down their length. Polypropylene FRP confined piles have higher load-bearing capacity than any other FRP composites. Moreover, the load transfer capacity calculated from the pile load test is moderately higher than the engineering news formula.

5. BIBLIOGRAPHY

[1] SHAIA, H., "*Behaviour of fiber reinforced polymer composite piles: experimental and numerical study*", D.Sc. Thesis, The University of Manchester, Manchester, 2013.

[2] GUADES, E., ARAVINTHAN, T., ISLAM, M., *et al*., "A review on the driving performance of FRP composite piles", *Composite Structures*, v. 94, n. 6, pp. 1932–1942, 2012. doi: http://dx.doi.org/10.1016/j.compstruct.2012.02.004.

[3] FENG, B., ZHU, Y.H., XIE, F., *et al*., "Experimental investigation and design of hollow section, centrifugal concrete filled GFRP tube columns", *Buildings*, v. 11, n. 12, pp. 598, 2021. doi: http://dx.doi.org/10.3390/buildings11120598.

[4] ALAMPALLI, S., O'CONNOR, J., YANNOTTI, A.P., *et al*. "FRPs for bridge construction and rehabilitation in New York", In: Bank, L.C. (ed), *Materials and construction: exploring the connection*, Reston, USA, ASCE, pp. 345–350, 1999.

[5] GRESIL, M., REVOL, V., KITSIANOS, K., *et al*., "Comparison between traditional non-destructive techniques and phase contrast X-ray imaging applied to aerospace carbon fiber reinforced polymer", *Applied Composite Materials*, v. 24, pp. 513–524, 2017. doi: http://dx.doi.org/10.1007/s10443-016-9540-1.

[6] TAIPALUS, R., HARMIA, T., FRIEDRICH, K., "Short fiber reinforced PP/PANI-Complex blends and their mechanical and electrical properties", *Applied Composite Materials*, v. 6, n. 3, pp. 167–175, 1999. doi: http://dx.doi.org/10.1023/A:1008858832318.

[7] CASSOL, D., RECH, G.L., THOMAZI, E., *et al*., "Influence of an over calcined calcium oxide-based shrinkagecompensating admixture on some properties of a self-compacting concrete", *Matéria (Rio de Janeiro)*, v. 27, n. 4, pp. e20220171, 2022. doi: http://dx.doi.org/10.1590/1517-7076-rmat-2022-0171.

[8] KUBOKI, T., GALLAGHER, E., JAR, P.Y., *et al*., "A new method to quantify delamination resistance of Fiber Reinforced Polymers (FRP) under transverse loading", *Applied Composite Materials*, v. 12, n. 2, pp. 93–108, 2005. doi: http://dx.doi.org/10.1007/s10443-004-6205-2.

[9] CHANG, L., ZHANG, Z., BREIDT, C., "Impact resistance of short fiber/particle reinforced epoxy", *Applied Composite Materials*, v. 11, n. 1, pp. 1–15, 2004. doi: http://dx.doi.org/10.1023/B:ACMA.0000003824.12136.25.

[10] SCHNEIDER, K., LAUKE, B., "Determination of compressive properties of fiber-reinforced polymers in the in-plane direction according to ISO 14126. Part 2: a critical investigation of failure behaviour", *Applied Composite Materials*, v. 14, n. 3, pp. 177–191, 2007. doi: http://dx.doi.org/10.1007/s10443-007-9039-x.

[11] ALSHIMMERI, A.J.H., JAAFAR, E.K., SHIHAB, L.A., *et al*., "Structural efficiency of non-prismatic hollow reinforced concrete beams retrofitted with CFRP sheets", *Buildings*, v. 12, n. 2, pp. 109, 2022. doi: http://dx.doi.org/10.3390/buildings12020109.

[12] KAW, A.K., *Mechanics of composite materials*, Boca Raton (FL), CRC Press, 2005.

[13] FAM, A.Z., RIZKALLA, S.H., "Flexural behavior of concrete-filled fiber-reinforced polymer circular tubes", *Journal of Composites for Construction*, v. 6, n. 2, pp. 123–132, 2002. doi: http://dx.doi.org/10.1061/(ASCE)1090-0268(2002)6:2(123).

[14] TUAKTA, C., "*Use of fiber reinforced polymer composite in bridge structures*", M.Sc. Thesis, Massachusetts Institute of Technology, Massachusetts, 2005.

[15] NANNI, A., BRADFORD, N.M., "FRP jacketed concrete under uniaxial compression", *Construction & Building Materials*, v. 9, n. 2, pp. 115–124, 1995. doi: http://dx.doi.org/10.1016/0950-0618(95)00004-Y.

[16] SAADATMANESH, H., EHSANI, M.R., LI, M.W., "Strength and ductility of concrete columns externally reinforced with fiber composite straps", *Structural Journal*, v. 91, pp. 434–447, 1994.

[17] MIRMIRAN, A., SHAHAWY, M., "A New concrete-filled hollow FRP composite column", *Composites. Part B, Engineering*, v. 27, n. 3-4, pp. 263–268, 1996. doi: http://dx.doi.org/10.1016/1359-8368(95)00019-4.

[18] FARDIS, M.N., KHALILI, H., "Concrete encased in fiberglass-reinforced plastic", *Journal Proceedings*, v. 78, pp. 440–446, 1981.

[19] AL ABADI, H., EL-NAGA, H.A., SHAIA, H., *et al*., "Refined approach for modelling strength enhancement of FRP-confined concrete", *Construction & Building Materials*, v. 119, pp. 152–174, 2016. doi: http://dx.doi.org/10.1016/j.conbuildmat.2016.04.119.

[20] HUANG, L., ZHANG, C., YAN, L., *et al*., "Flexural behavior of U-Shape FRP Profile-RC composite beams with inner GFRP tube confinement at concrete compression zone", *Composite Structures*, v. 184, pp. 674–687, 2018. doi: http://dx.doi.org/10.1016/j.compstruct.2017.10.029.

[21] HUANG, L., CHEN, L., YAN, L., *et al*., "Behavior of Polyester FRP tube encased recycled aggregate concrete with recycled clay brick aggregate: size and slenderness ratio effects", *Construction & Building Materials*, v. 154, pp. 123–136, 2017. doi: http://dx.doi.org/10.1016/j.conbuildmat.2017.07.197.

[22] ISKANDER, M.G., HASSAN, M., "State of the practice review in FRP composite piling", *Journal of Composites for Construction*, v. 2, n. 3, pp. 116–120, 1998. doi: http://dx.doi.org/10.1061/(ASCE)1090-0268(1998)2:3(116).

[23] SILVA, T.F., MOURA, M.A.D.N., SOUZA, E.D.F.C., *et al*., "Influence of the cooling process on the physicochemical properties of ladle furnace slag, used in the replacement of Portland cement", *Matéria (Rio de Janeiro)*, v. 27, n. 3, pp. e20220089, 2022. doi: http://dx.doi.org/10.1590/1517-7076-rmat-2022-0089.

[24] LEE, C., BONACCI, J.F., THOMAS, M.D., *et al*., "Accelerated corrosion and repair of reinforced concrete columns using carbon fiber reinforced polymer sheets", *Canadian Journal of Civil Engineering*, v. 27, n. 5, pp. 941–948, 2000. doi: http://dx.doi.org/10.1139/l00-030.

[25] GREEN, M.F., BISBY, L.A., FAM, A.Z., *et al*., "FRP confined concrete columns: behaviour under extreme conditions", *Cement and Concrete Composites*, v. 28, n. 10, pp. 928–937, 2006. doi: http://dx.doi.org/10.1016/j.cemconcomp.2006.07.008.

[26] SHAMSUDDOHA, M., ISLAM, M.M., ARAVINTHAN, T., *et al*., "Effectiveness of using fiber-reinforced polymer composites for underwater steel pipeline repairs", *Composite Structures*, v. 100, pp. 40–54, 2013. doi: http://dx.doi.org/10.1016/j.compstruct.2012.12.019.

[27] AL-ROUSAN, R., NUSIER, O., ABDALLA, K., *et al*., "NLFEA of sulfate-damaged circular CFT steel columns confined with CFRP composites and subjected to axial and cyclic lateral loads", *Buildings*, v. 12, n. 3, pp. 296, 2022. doi: http://dx.doi.org/10.3390/buildings12030296.

[28] LI, W., WEN, F., ZHOU, M., *et al*., "Assessment and prediction model of GFRP bars' durability performance in seawater environment", *Buildings*, v. 12, n. 2, pp. 127, 2022. doi: http://dx.doi.org/10.3390/buildings12020127.

[29] EULER, S.A.J., BARATA, M.S., SECCO, P., *et al*., "The use of red mud and kaolin waste in the production of a new building material: pozzolanic pigment for colored concrete and mortar", *Matéria (Rio de Janeiro)*, v. 27, n. 3, pp. e20220149, 2022.

[30] TRIANTAFYLLOU, G., ROUSAKIS, T., KARABINIS, A., "Corroded RC beams at service load before and after patch repair and strengthening with NSM CFRP strips", *Buildings*, v. 9, n. 3, pp. 67, 2019. doi: http://dx.doi.org/10.3390/buildings9030067.

[31] HAN, J., FROST, J.D., "Buckling of vertically loaded fiber-reinforced polymer piles", *Journal of Reinforced Plastics and Composites*, v. 18, n. 4, pp. 290–318, 1999. doi: http://dx.doi.org/10.1177/073168449901800401.

[32] SAKR, M., EL NAGGAR, M.H., NEHDI, M., "Wave equation analyses of tapered FRP-concrete piles in dense sand", *Soil Dynamics and Earthquake Engineering*, v. 27, n. 2, pp. 166–182, 2007. doi: http://dx.doi.org/10.1016/j.soildyn.2005.11.002.

[33] BROMS, B.B., "Lateral resistance of piles in cohesionless soils", *Journal of the Soil Mechanics and Foundations Division*, v. 90, n. 3, pp. 123–158, 1964. doi: http://dx.doi.org/10.1061/JSFEAQ.0000614.

[34] MEYERHOF, G.G., "Behaviour of pile foundations under special loading conditions: 1994 RM hardy keynote address", *Canadian Geotechnical Journal*, v. 32, n. 2, pp. 204–222, 1995. doi: http://dx.doi.org/10.1139/t95-024.

[35] GIRALDO VALEZ, J., RAYHANI, M.T., "Axial and lateral load transfer of fibre-reinforced polymer (FRP) piles in soft clay", *International Journal of Geotechnical Engineering*, v. 11, n. 2, pp. 149–155, 2017.

[36] GIRALDO, J., RAYHANI, M.T., "Load transfer of hollow Fiber-Reinforced Polymer (FRP) piles in soft clay", *Transportation Geotechnics*, v. 1, n. 2, pp. 63–73, 2014. doi: http://dx.doi.org/10.1016/j.trgeo.2014.03.002.